

Fig. 4. Return loss vs Freq. plots of different Iterations from stage-1 to stage-6.

#### IV. RESULTS AND DISCUSSIONS

##### A. Reflection Coefficient of the Proposed Antenna

The reflection coefficient, which is a critical parameter in antenna assessment, is analyzed by employing an iterative design method as shown in Fig. 4. The proposed antenna's initial iteration features are a central 2.4 GHz resonance frequency and a significant bandwidth of 100MHz. The antenna produces even more improvement

in the second iteration by achieving an enhanced bandwidth of 110 MHz at a resonant frequency of 2.3 GHz.

The design exhibits remarkable dual-band behavior at the third iteration with frequencies of 1.6 GHz and 2.3 GHz of resonance. The fourth and fifth rounds of the iterative refining process take an interesting turn when a circular-shape etched patch using the Kotch fractal is inserted. This new adjustment leads to a significant bandwidth gain and the appearance of a multiband phenomenon. Resonating frequencies of 1.7 GHz, 2.3 GHz,

and 3.87 GHz are now shown by the antenna, demonstrating the effectiveness of the iterative design

process and the special roles played by the Kotch fractal in determining the antennas performance characteristics.

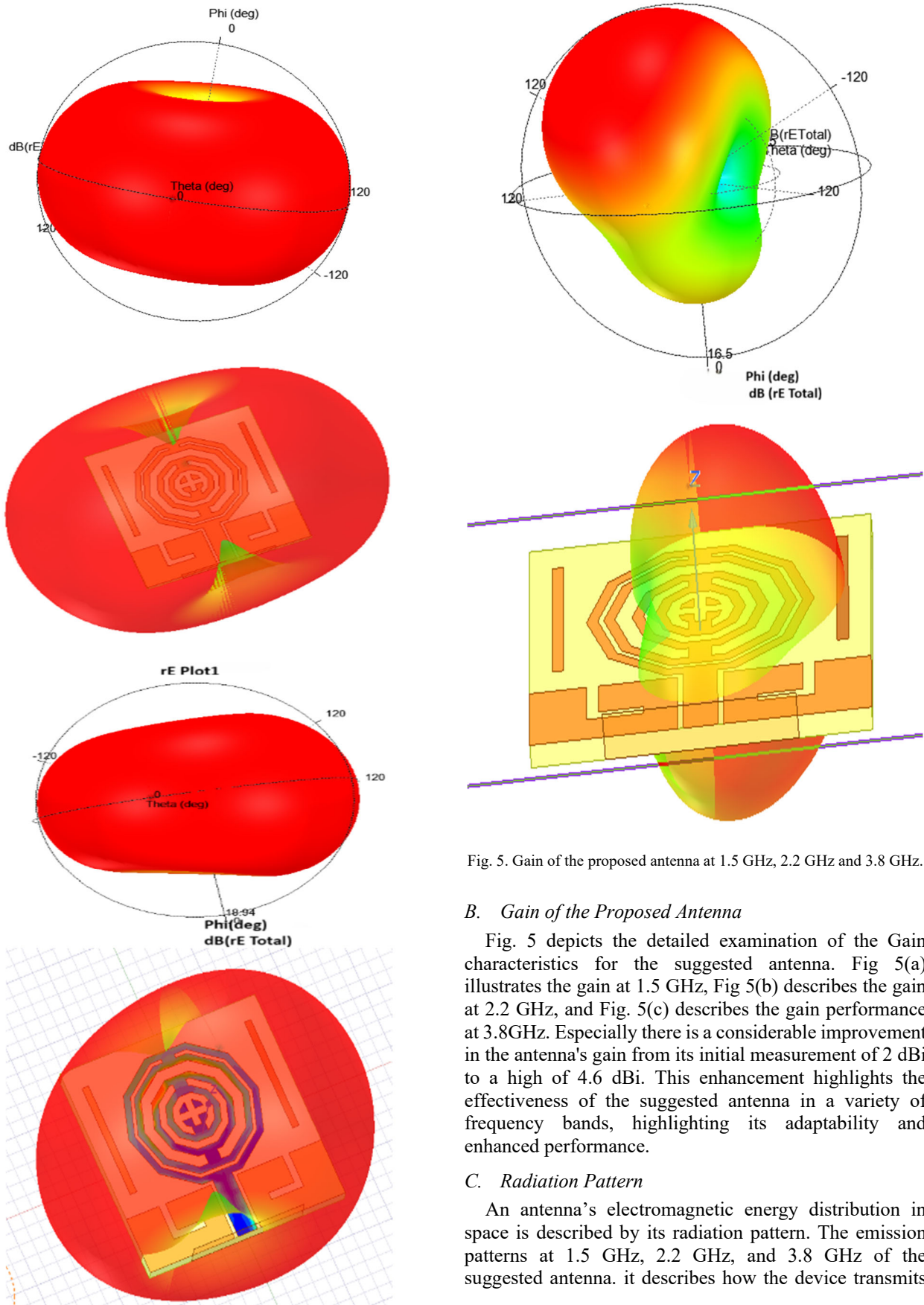


Fig. 5. Gain of the proposed antenna at 1.5 GHz, 2.2 GHz and 3.8 GHz.

**B. Gain of the Proposed Antenna**

Fig. 5 depicts the detailed examination of the Gain characteristics for the suggested antenna. Fig 5(a) illustrates the gain at 1.5 GHz, Fig 5(b) describes the gain at 2.2 GHz, and Fig. 5(c) describes the gain performance at 3.8GHz. Especially there is a considerable improvement in the antenna's gain from its initial measurement of 2 dBi to a high of 4.6 dBi. This enhancement highlights the effectiveness of the suggested antenna in a variety of frequency bands, highlighting its adaptability and enhanced performance.

**C. Radiation Pattern**

An antenna's electromagnetic energy distribution in space is described by its radiation pattern. The emission patterns at 1.5 GHz, 2.2 GHz, and 3.8 GHz of the suggested antenna. it describes how the device transmits

and receives electromagnetic waves at these particular frequencies as depicted in Fig. 6.

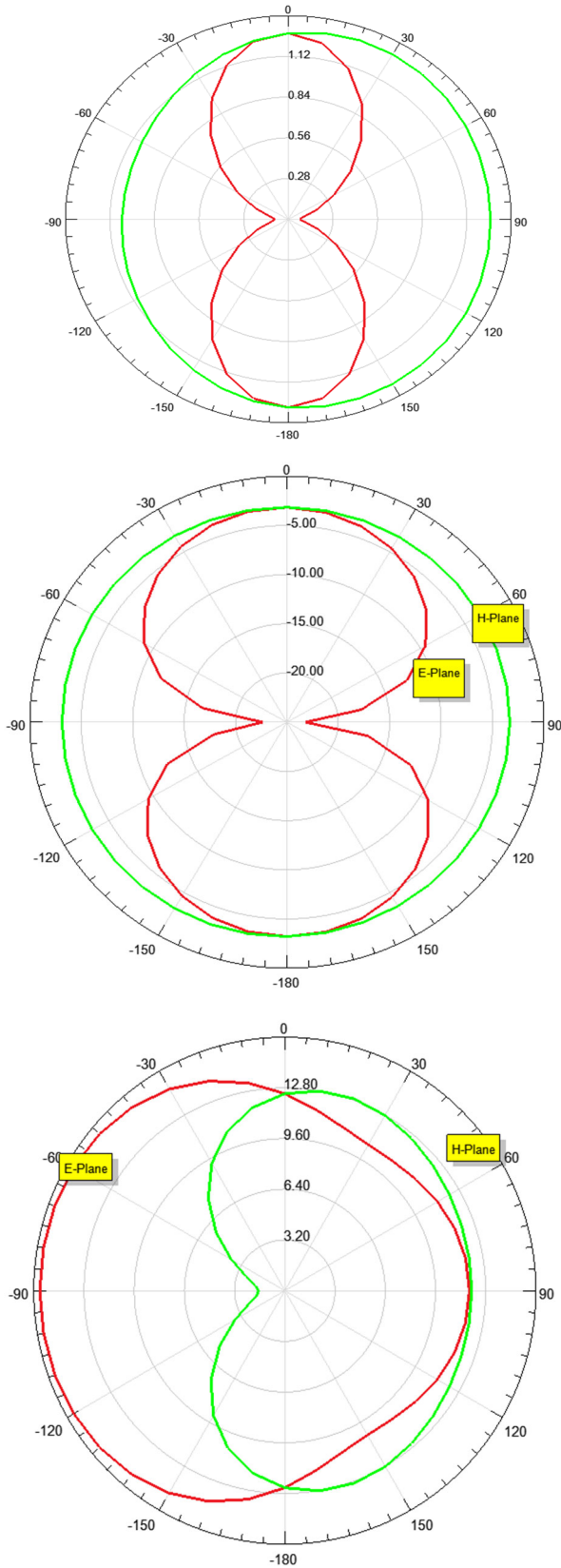
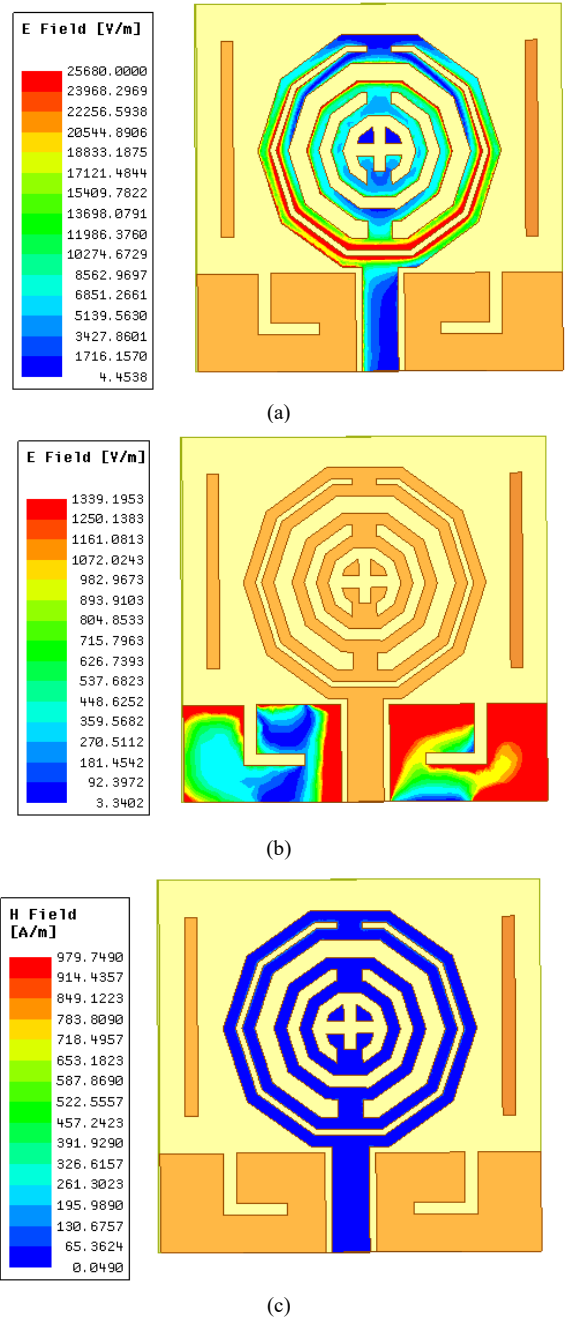


Fig. 6. Radiation pattern of the proposed antenna at 1.5 GHz, 2.2 GHz and 3.8 GHz.

The radiation pattern of the proposed antenna illustrates the geographical distribution of energy radiated at 1.5 GHz frequency. This pattern proves the coverage and directivity of the antenna propagates electromagnetic waves in all directions.

The radiation pattern changes when changes are made to 2.2 GHz to correspond with the antenna's characteristics at this higher frequency. Changes in the pattern indicate adjustments made to the antenna's beam width, side lobes, and radiation efficiency overall.

The radiation pattern further adjusts to the unique properties of this frequency at 3.8 GHz. Understanding the pattern at this frequency is essential to evaluate the antenna's performance at high-frequency applications, since several design factors such as height, length and width of the antenna are involved.



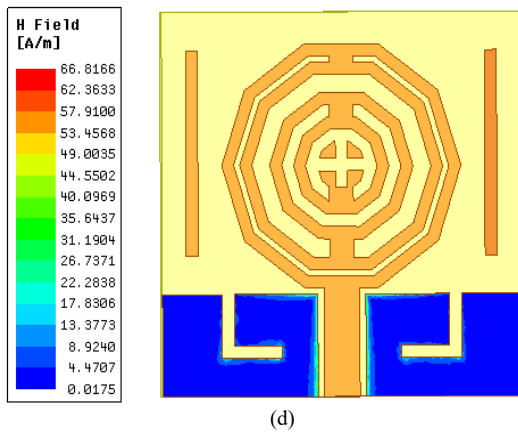


Fig. 7. represents the E-field and H-field of the proposed antenna: (a). E Field of the main patch, (b). E Field of the ground and parasitic elements, (c). H Field of the main patch, (d). H Field of the ground.

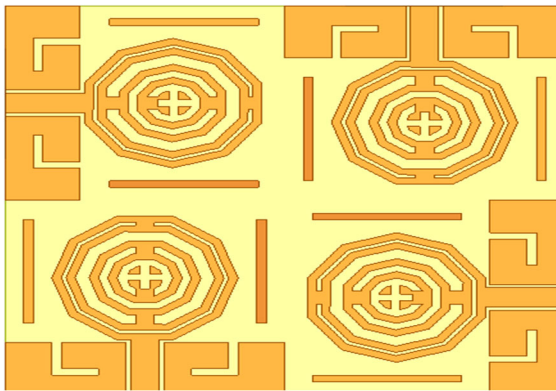


Fig. 8. Geometrical view of the proposed antenna.

#### D. Current Distribution

Fig. 7 gives the current distribution of the single patch antenna. As seen in Fig. 8, this low-loss characteristic is maintained for every port, confirming the antenna's reliable operation. In addition, the antenna has a

remarkable bandwidth of 500MHz in three different frequency bands, which enhances its adaptability and efficiency in a variety of operational situations. The S-parameter plot of the antenna is depicted in Fig. 9, providing important details about its performance attributes. The suggested antenna is noteworthy for having a very low reflection coefficient; it reaches  $-30$  dB which indicates very little signal loss.

The antenna is carefully crafted from FR4 (flame retardant) material by choosing a dielectric constant of 4.4 with a loss tangent of 0.02 for maximum performance as shown in the Fig. 10. Measuring  $60 \times 60 \times 1.6$  mm, its proportions serve a variety of purposes, including LTE, Wi-Fi, INSAT, GPS (global positioning system), and vehicular communication. Across a range of communication and navigation systems, this thoughtful design guarantees adaptability and efficiency.

#### E. Envelope Correlation Coefficient (ECC)

The envelope correlation coefficient of 0.01 is measured during testing to assess amplitude changes across the four ports of the proposed antenna, which is shown in Fig. 11. This indicates that there are no connections between the amplitude fluctuations at each port of the antenna, indicating effective spatial diversity and pointing to the possibility of better MIMO system performance.

#### F. Diversity Gain

The relationship between a MIMO antenna system's diversity gain and its envelope correlation coefficient (ECC) value is often inverse. According to the observations from Fig. 12, the suggested MIMO antenna has a notable diversity gain of 10. This demonstrates how using several channels or pathways inside the antenna system may effectively increase reliability and performance, especially in demanding communication scenarios.

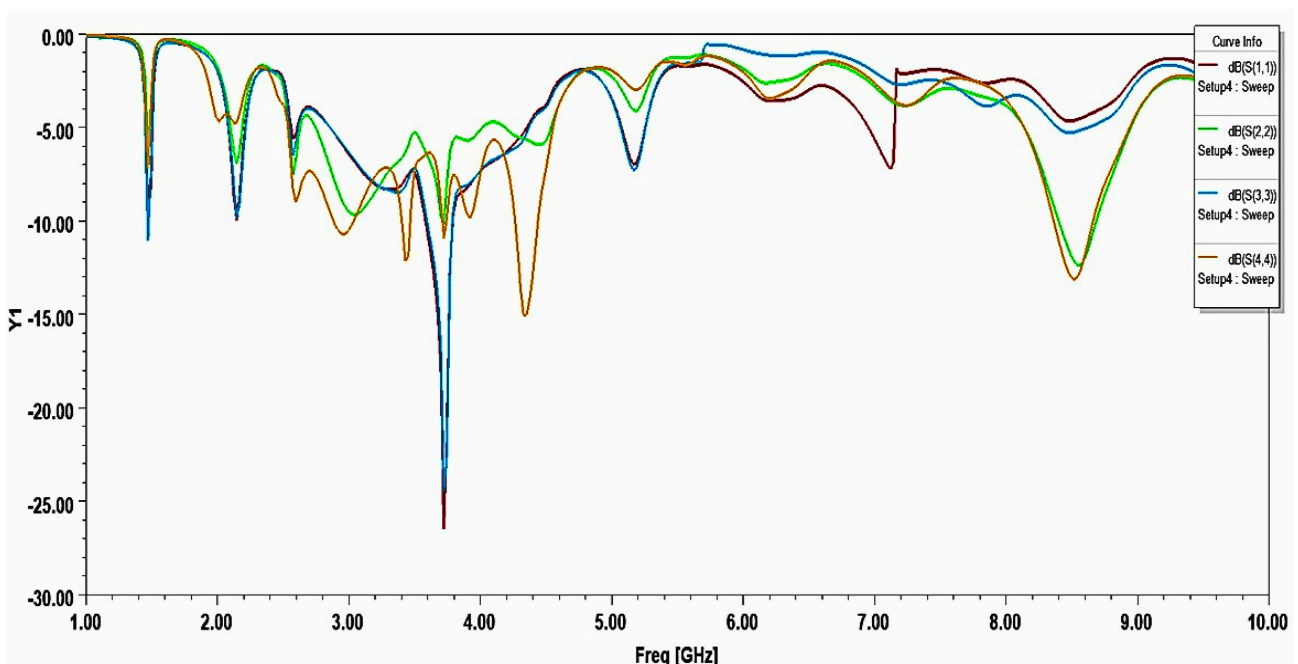


Fig. 9. The S-parameter of the proposed antenna.

G. Antenna Installed on the Car's Roof

The suggested antenna is positioned on the car's roof in a manner that, as depicted in Fig. 13, results in an electrical size significantly larger than the antenna's physical dimensions. The analysis also takes into account situations in which the antenna is fixed to the vehicle's front bumper. The simulations to assess the antenna's performance in different locations are meticulously conducted using the ANSYS HFSS 2019 R2 version.

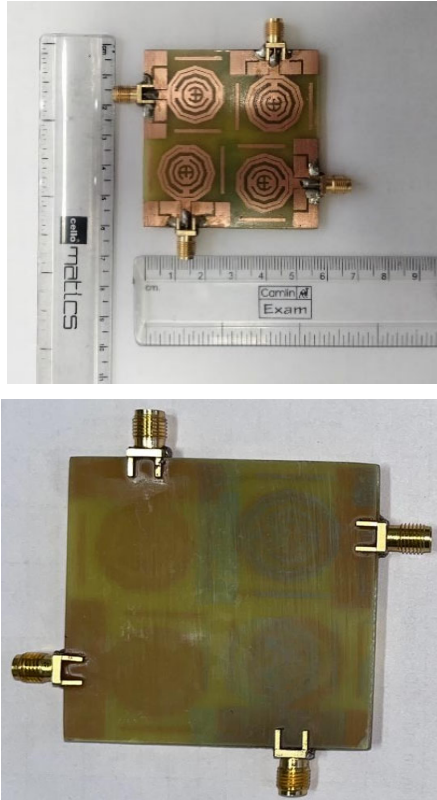


Fig. 10. Fabricated model of the designed antenna (Top & Bottom).

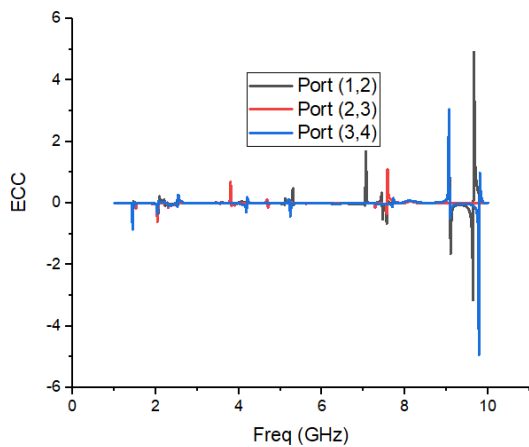


Fig. 11. ECC value of the proposed antenna.

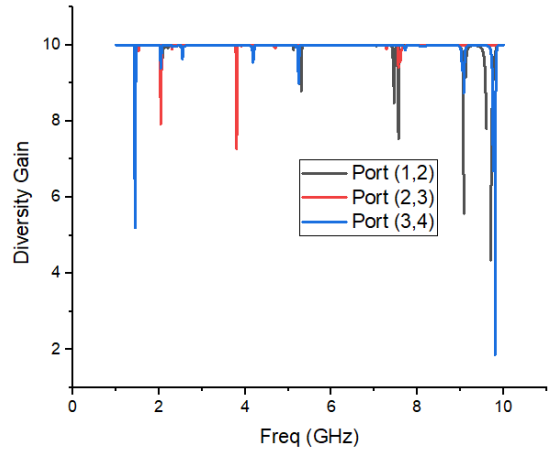


Fig. 12. Diversity gains plot of the proposed antenna.

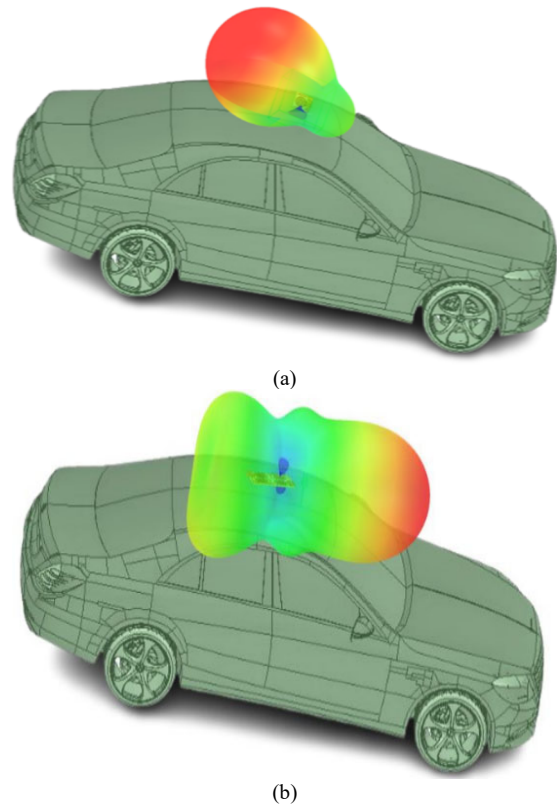


Fig. 13. Antenna installed on the roof of the car: (a). Using a single element, (b) Using a MIMO arrangement.

H. Comparison of Simulated Proposed with Existing different Antennas

Table III presents a comparative analysis between the proposed antenna at different stages. Table IV presents a comparative analysis between the proposed antenna and existing works. After mounting the suggested antenna on the vehicle's roof, the measured gain was 4.6 dBi. In addition, the antenna's remarkable 80% radiation efficiency was noted, confirming its efficiency once it was mounted on the car's roof (see Fig. 14).

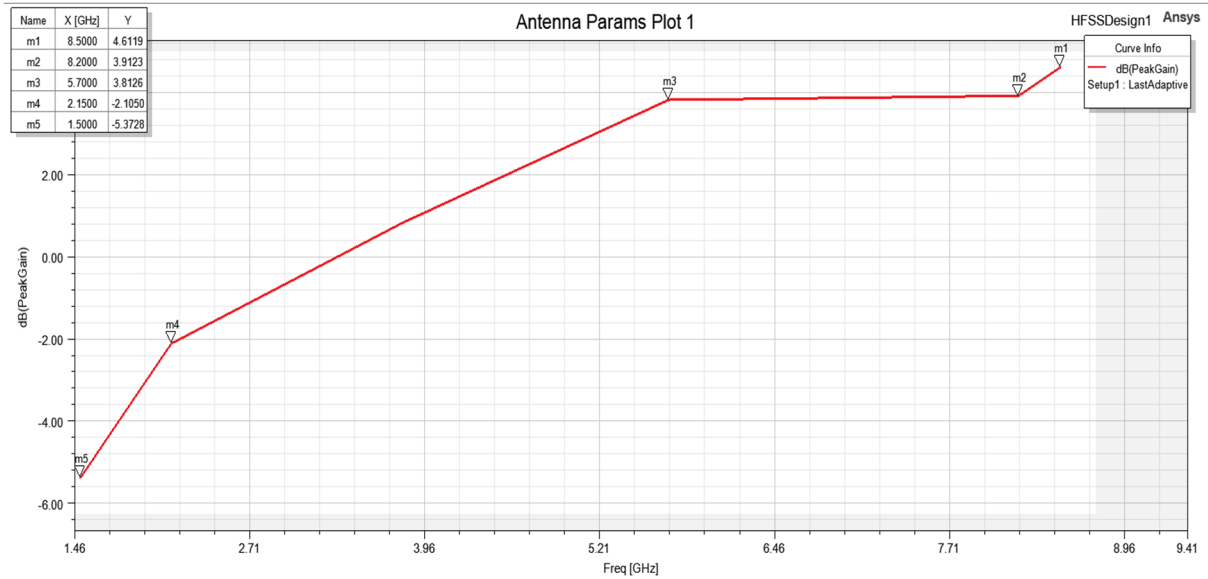
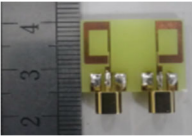
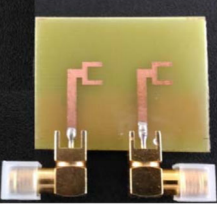

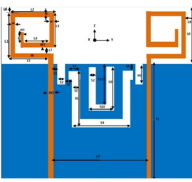


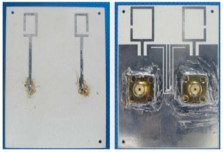

Fig. 14. Measured gain of MIMO antenna against frequency.

TABLE III. COMPARISON OF THE PROPOSED ANTENNA AT DIFFERENT STAGES

Parameter Iteration wise	S11 (dB)	VSWR	Bandwidth (MHz)	Gain (dB)	Efficiency (%)
Stage-1	-18	1.07	100	3.2	60
Stage-2	-23	1.08	110	1.1	70.2
Stage-3	-24	1.05	50, 120	2.2, 1.1	72
Stage-4	-25	1.1	100, 110, 200	3.1, 1.2, 2.2	73
Stage-5	-23	1.2	100, 110, 200	3.2, 1.1, 2.2	75
Stage-6	-35	1.1	100, 110, 500	3.2, 1.13, 4.6	87

TABLE IV. COMPARISON OF PROPOSED ANTENNA WITH OTHER ANTENNAS

Ref No.	Patch	Dimensions	Substrate Material	Operating Frequency	Gain	Efficiency
[23]		15.5 × 18 x 1.6 mm <sup>3</sup>	FR4	2.41 GHz	0.72 dBi	78%
[24]		26 x 34 x 0.8 mm <sup>3</sup>	FR4	2.5-10.7 GHz	4.3 dBi	80%
[25]		28 × 31 × 0.8 mm <sup>3</sup>	FR4	4.7-10 GHz	1.7-4.2 dBi	60%
[26]		70 × 70 × 0.8mm <sup>3</sup>	FR4	1.2 GHz	2.5 dBi	-

[27]		$50 \times 17 \times 0.8 \text{ mm}^3$	CEM-1 S3110	1.5, 2, 2.5, 5 & 7 GHz	2 dBi	70%
Proposed work		$60 \times 60 \times 1.6 \text{ mm}^3$	FR4	1.5/ 2.6/3.7/4/ 7.2/8.2/8.7 GHz	4.6 dBi	87%

## V. CONCLUSION

The proposed antenna design constitutes a triple-band decagon-shaped antenna suitable for applications such as GPS (Global Positioning System), LTE, Wi-Fi, and vehicle communication. The antenna is built on a  $30 \times 30 \times 1.6 \text{ mm}^3$  FR-4 substrate and has resonance frequencies of 1.5 GHz, 2.2 GHz, and 3.8 GHz. Comparable respective maximum gains are  $-3.2 \text{ dB}$ ,  $1.13 \text{ dB}$ , and  $3 \text{ dB}$ , in that order. The antenna achieves simulated radiation efficiencies ranging from 60% in baseline designs to 75% after incorporating the metasurface structure, while measured efficiencies of the MIMO antenna mounted on a vehicle roof reach 87%. Likewise, the peak gain of 4.6 dBi reported corresponds to the measured value obtained after prototype fabrication and vehicle mounting, demonstrating a significant improvement over initial simulated gain of approximately 2 dBi. Notably, at 2.2 GHz, a maximum radiation efficiency of 75% is attained. Moreover, the suggested MIMO antenna design exhibits resonance across a wide frequency ranging from 1.5 GHz to 8.7 GHz and achieves a remarkable peak gain of 4.6 dBi and an exceptional radiation efficiency of 87%. These simulations included the examination of scattering parameters, 2D/3D radiation pattern plots, and surface current distribution. To confirm the simulation results, practical return loss characteristics were tested under appropriate conditions

## CONFLICTS OF INTEREST:

The authors declare no conflict of interest.

## AUTHOR CONTRIBUTIONS

Akansha Gupta and Purnima K Sharma were primarily responsible for drafting the main manuscript text, conducting literature research, methodology, and organizing the content; T. J. V. Subrahmanyeswara Rao and T. V. N. L. Aswini were actively involved in the practical aspects of the research, specifically in antenna fabrication and testing; Dinesh Sharma contributed to the review process by providing valuable insights and recommendations; all authors had approved the final version.

## REFERENCES

- [1] M. F. Tufvesson, J. Karedal, and C. Mecklenbräuker, "A survey on vehicle-to-vehicle propagation channels," *IEEE Wireless Commun.*, vol. 16, no. 6, pp. 12–22, 2009.
- [2] S. Arumugam, S. Manoharan, S. K. Palaniswamy, and S. Kumar, "Design and performance analysis of a compact quad-element UWB MIMO antenna for automotive communications," *Electronics*, vol. 10, 2021.
- [3] V. Saritha and C. Chandrasekhar, "A conformal multi-band MIMO antenna for vehicular communications," *Progress in Electromagnetics Research Letters*, vol. 108, pp. 49–57, 2023.
- [4] M. Kanagasabai, S. Shanmuganathan, M. G. N. Alsath, and S. K. Palaniswamy, "A novel low-profile 5G MIMO antenna for vehicular communication," *International Journal of Antennas and Propagation*, October 2022.
- [5] B. T. Madhav, T. Anilkumar, and S. K. Kotamraju, "Transparent and conformal wheelshaped fractal antenna for vehicular communication applications," *AEU-International Journal of Electronics and Communications*, vol. 91, pp. 1–10, Jul. 1, 2018.
- [6] D. S. Woo, "A triple band C-shape monopole antenna for vehicle communication application," *Progress in Electromagnetics Research C*, vol. 121, pp. 97–106, 2022.
- [7] M. P. Joshi and V. J. Gond, "Design and analysis of microstrip patch antenna for WLAN and vehicular communication," *Progress in Electromagnetics Research C*, vol. 97, pp. 163–176, 2019.
- [8] C. T. P. Song, P. S. Hall, and H. G. Shiraz, "Multiband multiple ring monopole antennas," *IEEE Transactions on Antennas and Propagation*, vol. 51, no. 4, April 2003.
- [9] P. Iyampalam and I. Ganesan, "Meta-material inspired penta-band decagon fractal antenna for wireless applications, e-Prime," *Advances in Electrical Engineering, Electronics and Energy*, vol. 6, 2023.
- [10] K. Patchala, Y. R. Rao and A. M. Prasad, "Triple band notch compact MIMO antenna with defected ground structure and split ring resonator for wideband applications," *Heliyon*, vol. 6, 2020.
- [11] Y. Zheng, P. Wang, M. Hua, and P. Gao, "Compact triple-band monopole antenna for WLAN/WiMAX applications," *IEICE Electron. Express*, vol. 10, 2013.
- [12] P. C. Ooi and K. T. Selvan, "The effect of ground plane on the performance of a square loop CPW-Fed printed antenna," *Prog. Electromagnetics Research Letters*, vol. 19, pp. 103–111, 2010.
- [13] A. Subbarao and S. Raghavan, "Compact coplanar waveguide-fed planar antenna for ultra-wideband and WLAN applications," *Wireless Pers Commun*, vol 71, pp. 2849–2862, 2013.
- [14] R. T. R. Rao, "Design and performance analysis of a penta-band spiral antenna for vehicular communications," *Wireless Pers Commun*, vol 96, pp. 3421–3434, 2017.
- [15] T. Mondal, S. Samanta, R. Ghatak, and S. R. B. Chaudhuri, "A novel tri-band hexagonal microstrip patch antenna using modified sierpinski fractal for vehicular communication," *Progress in Electromagnetics Research C*, vol 57, pp. 25–34, 2015.
- [16] W. Lee, Y. K. Hong, J. J. Lee, J. H. Park, and W. Seong, "Omnidirectional low-profile multiband antenna for vehicular telecommunication," *Progress in Electromagnetics Research Letters*, vol. 51, pp. 53–59, 2015.

- [17] M. Q. Abdalrazak, A. H. Majeed, and R. A. A. Alhameed, "An analytical investigation on the performance of 1D and 2D antenna arrays for MM-Wave modern communication systems," *Iraqi Journal of Information & Communications Technology*, vol. 6, no. 2, pp. 78–88, 2023.
- [18] P. K. Sharma, D. Sharma, T. J. V. S. Rao, J. R. Szymański, M. Ż. Mortka, and M. Sathiyarayanan, "Design and implementation of a meta-material based ultra-wide band microstrip patch antenna for vehicular communication," *Microsystem Technologies*, 2024
- [19] P. K. Sharma, J. R. Szymański, M. Ż. Mortka, M. Sathiyarayanan, and D. Sharma, "Design and analysis of four-leaf clover shaped MIMO antenna for Sub-6 GHz V2X applications," *Frequenz*, vol. 78, pp. 347–362, 2024.
- [20] S. Rajasri and R. B. Rani, "Design and performance analysis of metamaterial-inspired decagon-shaped antenna for vehicular communications," *Progress in Electromagnetics Research Letters*, vol. 105, pp. 139–147, 2022.
- [21] I. Bulu, H. Caglayan, K. Aydin, and E. Ozbay, "Compact size highly directive antennas based on the SRR metamaterial medium," *New Journal of Physics*, vol. 7, 2005.
- [22] H. M. Marhoon, H. A. Abdalnabi, and Y. Y. A. Aboosi, "Designing and analysing of a modified rectangular microstrip patch antenna for microwave applications," *Journal of Communications*, vol. 17, no. 8, pp. 668–674, 2022.
- [23] L. S. Yang, T. Li, and S. Yan, "Highly compact MIMO antenna system for LTE/ISM applications," *International Journal of Antennas and Propagation*, 2015.
- [24] J. C. Rao and N. Venkateswara Rao, "Compact UWB MIMO slot antenna with defected ground structure," *ARPJ. Eng. Appl. Sci.*, vol. 11, no. 17, 2016.
- [25] J. Ren *et al.*, "Compact printed MIMO antenna for UWB applications," *IEEE Antennas and Wireless Propagation Letters*, vol. 13, 2014.
- [26] F. Ahmed, H. M. Chowdhury, and A. A. Rahman, "A multiband MIMO antenna for future generation handset applications," in *Proc. International Conference on Electrical, Computer and Communication Engineering (ECCE)*, 2017, pp. 16–18, 2017.
- [27] X. Zhou, X. L. Quan, and R. L. Li, "A dual-broadband MIMO antenna system for GSM/UMTS/LTE and WLAN handsets," *IEEE Antennas and Wireless Propagation Letters*, vol. 11, 2012.

Copyright © 2026 by the authors. This is an open access article distributed under the Creative Commons Attribution License which permits unrestricted use, distribution, and reproduction in any medium, provided the original work is properly cited ([CC BY 4.0](https://creativecommons.org/licenses/by/4.0/)).